

## Size Effect of Mesoporous Organosilica Nanoparticles on Penetration and Accumulation for

### Tumor

*Junjie Zhang,<sup>a</sup> Xiaofen Wang,<sup>b</sup> Jun Wen,<sup>c</sup> Xiaodan Su,<sup>a</sup> Lixing Weng,<sup>a</sup> Jintao Li,<sup>e</sup> Chunyan Wang,<sup>b</sup> Ying Tian,<sup>b</sup> Yunlei Zhang,<sup>b</sup> Jun Tao,<sup>a</sup> Peng Xu,<sup>d</sup> Lianhui Wang,<sup>\*a</sup> Guangming Lu,<sup>b</sup> and Zhaogang Teng<sup>\*a,b</sup>*

<sup>a</sup> Key Laboratory for Organic Electronics and Information Displays & Institute of Advanced Materials (IAM), Nanjing University of Posts & Telecommunications, Nanjing, 210046 Jiangsu, P. R. China

Email: [iamlhwan@njupt.edu.cn](mailto:iamlhwang@njupt.edu.cn)

Email: [iamzgteng@njupt.edu.cn](mailto:iaczgteng@njupt.edu.cn)

<sup>b</sup> Department of Medical Imaging, Jinling Hospital, School of Medicine, Nanjing University, Nanjing, 210002 Jiangsu, P. R. China

<sup>c</sup> Department of Medical Imaging, Affiliated Hospital of Nanjing University of Chinese Medicine, Nan Jing, 210002 Jiangsu, P. R. China

<sup>d</sup> College of Chemical Engineering, Nanjing Forestry University, Nanjing, 210037 Jiangsu, P.R. China

<sup>e</sup> College of Computer and Information, Hohai University, 210098 Jiangsu, P. R. China

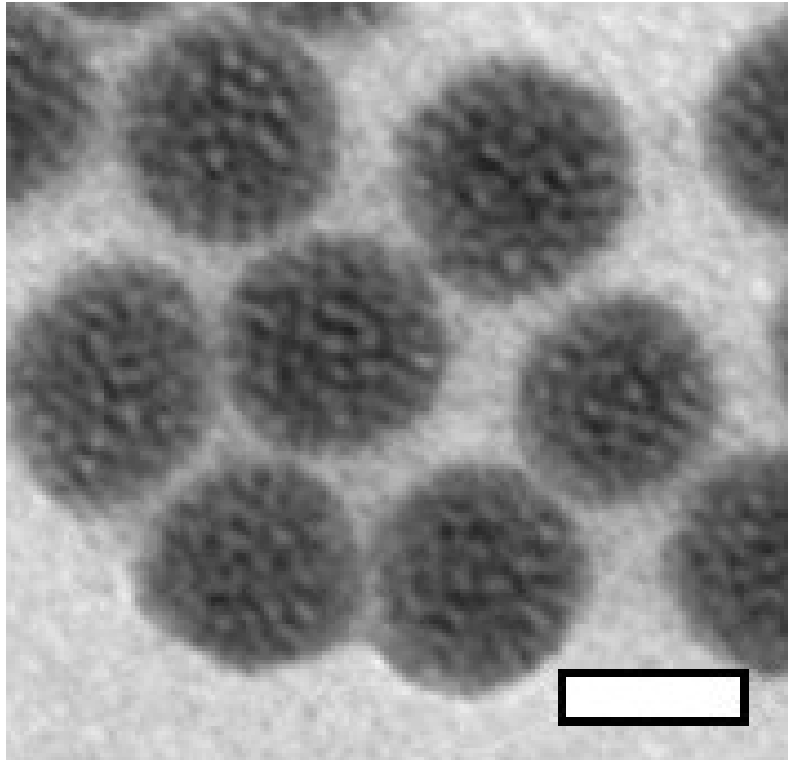


**Figure S1.** High magnification TEM image of the 60-nm MONs. scale bar: 50 nm.

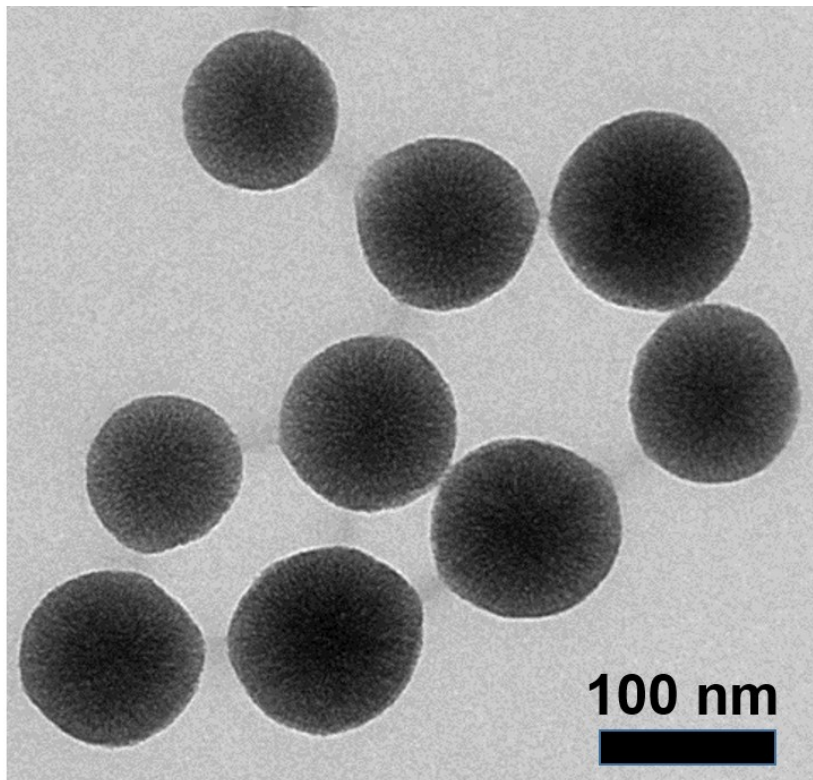


**Figure S2.** High magnification TEM image of the 100-nm MONs.

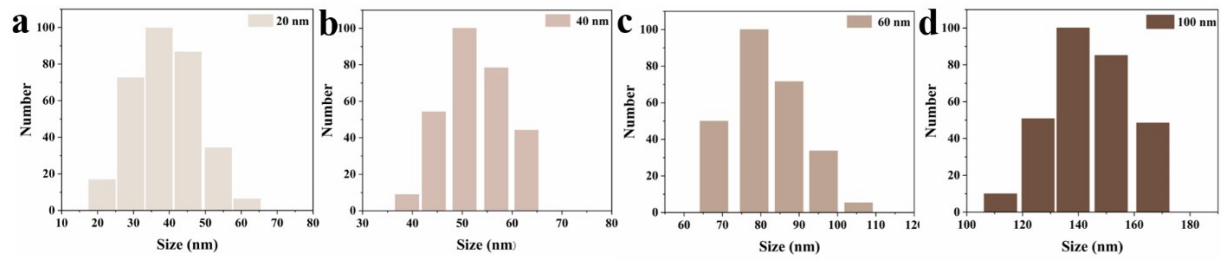


**Figure S3.** The hydrodynamic size distributions in DMEM containing 10% FBS.

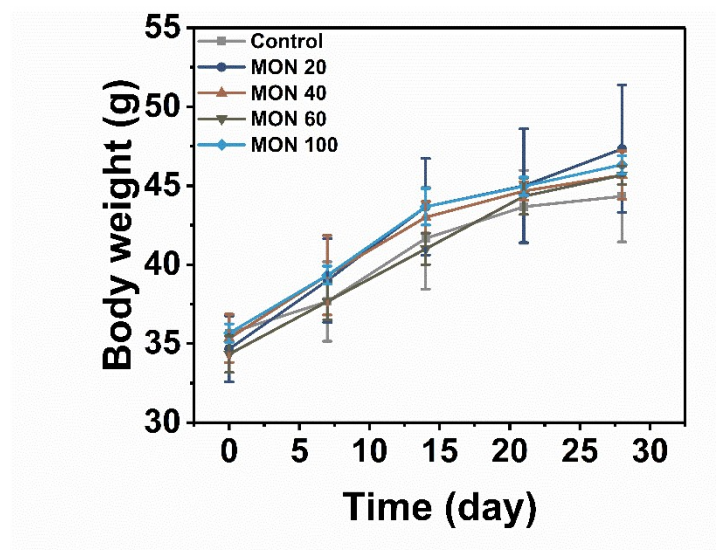


**Figure S4.** Weight change of the MON-treated mice 30 days post-injection at a dose of 5 mg kg<sup>-1</sup>.

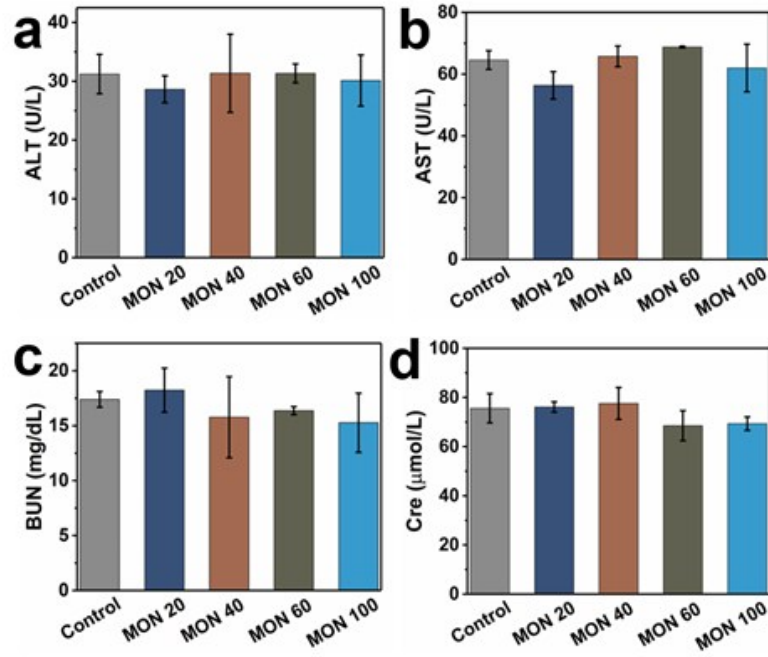


**Figure S5.** Serum biochemical analysis of the mice after injection with different-sized MONs at a dose of 5 mg/kg. The measures include ALT, AST, BUN, and Cre.

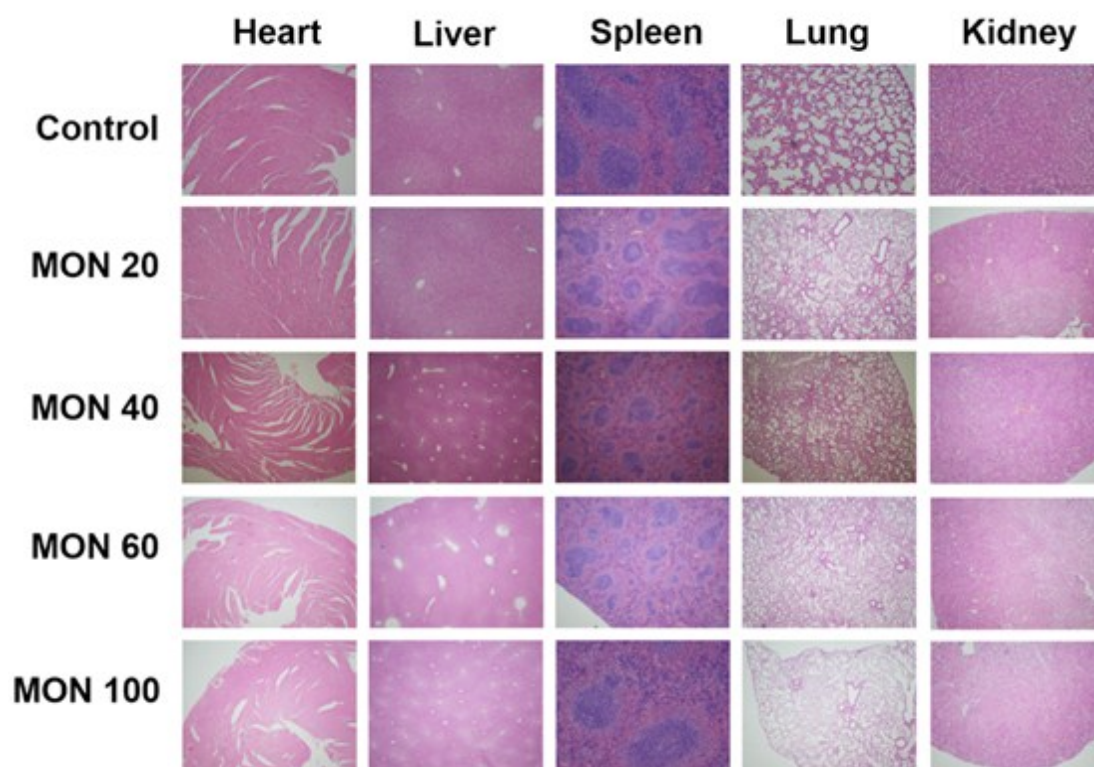


**Figure S6.** Histological images of the major organs of mice after intravenous administration of different-sized MONs at a dose of 5 mg kg<sup>-1</sup> at 30 days postinjection. All images shown are of 100× magnification.

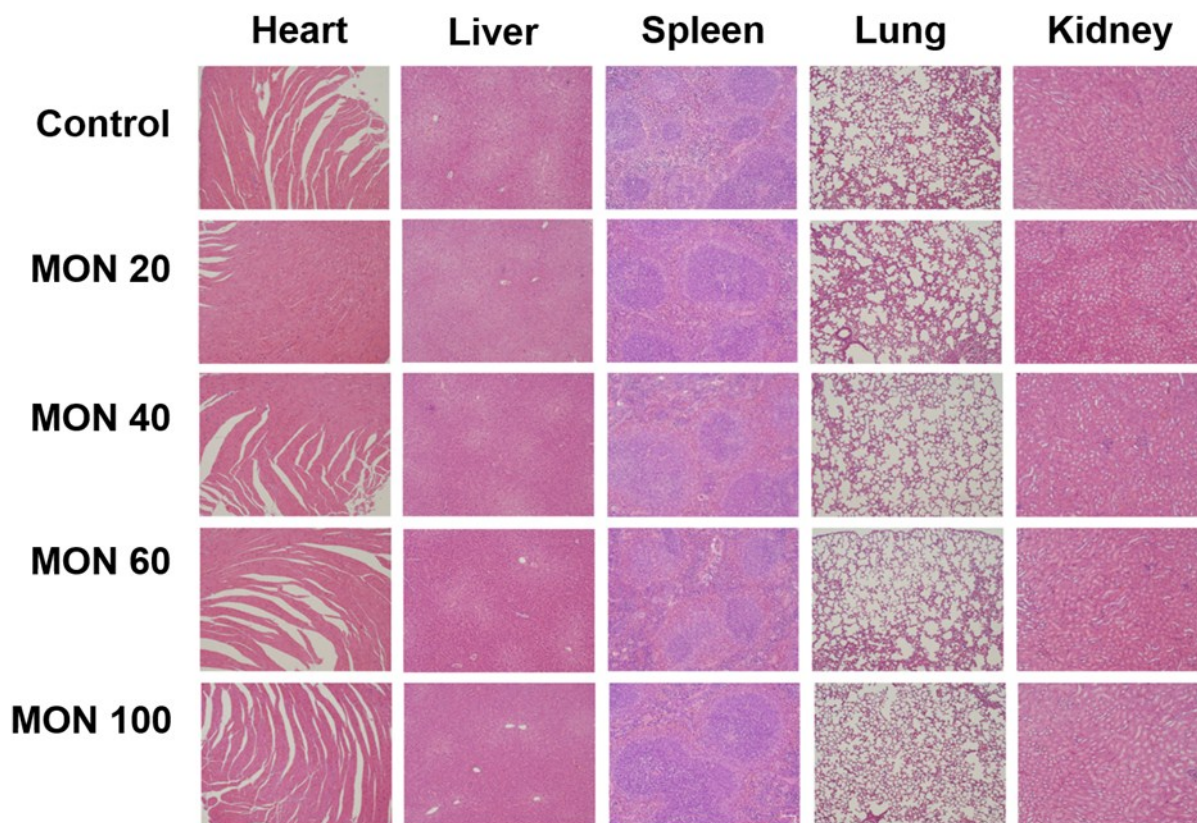


**Figure S7.** Histological images of the major organs of mice after intravenous administration of different-sized MONs at a dose of 20 mg kg<sup>-1</sup> at 30 days postinjection. All images shown are of 100× magnification.

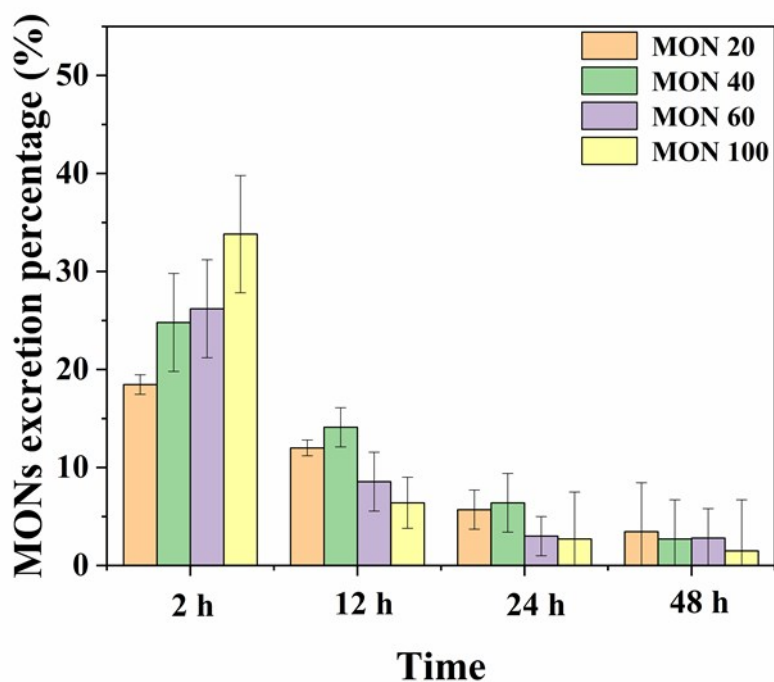


**Figure S8.** Excretion percentages of the MONs of different particle sizes in urine of ICR mice after tail intravenous injection. Male ICR mice were randomly separated into four groups ( $n = 5$ ) and intravenously injected with MONCs (MON-Cy5.5) at doses of  $5 \text{ mg kg}^{-1}\text{d}$ . At 2, 12, 24 and 48 h, liquid urine ( $50 \text{ }\mu\text{L}$ ) was mixed with cool methanol ( $450 \text{ }\mu\text{L}$ ) to determine the fluorescence intensity ( $A_u$ , in count per mg urine) and protein concentration of urine ( $C_p$ , in mg protein per mg urine). The protein content in urine (expressed by  $C_p$ ) was measured by the Bradford method using a Bradford Protein Assay Kit, which was purchased from Nanjing KeyGen Biotech Co. Ltd. (Nanjing, China). Furthermore, the sample percentages in each urine specimen ( $P_{s\_urine}$ , in %) could be calculated according to the volume of urine ( $V_{urine}$ , in mL), the protein concentration in urine ( $C_{p\_urine}$ , in mg protein per mL urine), the fluorescence density of each sample in urine ( $A_{s\_urine} = A_u/C_{p\_urine}$ , in count per mg protein), and the fluorescence intensity of each unit mass sample ( $A_{s0}$ , in count per  $\mu\text{g}$  MONs), namely  $P_{s\_urine} = C_{p\_urine} \times V_{urine} \times A_{s\_urine} / A_{s0}$ .

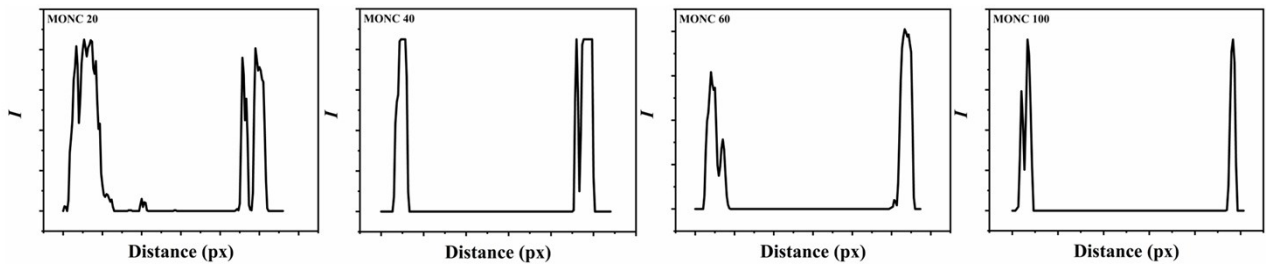


**Figure S9.** Fluorescent linear profiles of the U87MG MCSs at a depth of 120  $\mu\text{m}$  after incubating with different sized MONs for 4 h.

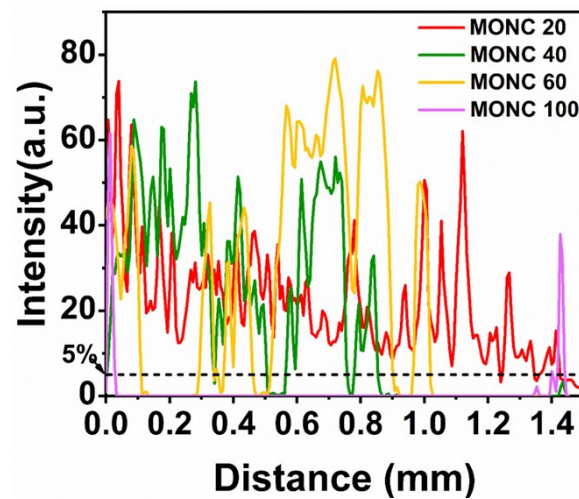


**Figure S10.** Tumor penetration depth analysis. The profile lines show the fluorescence changes from the tumor periphery to the interior as shown in Figure 4g.